

On the interaction between Autonomous Mobility-on-Demand systems and the power network: models and coordination algorithms

Federico Rossi, Ramon Iglesias, Mahnoosh Alizadeh, and Marco Pavone

Abstract—We study the interaction between a fleet of electric, self-driving vehicles servicing on-demand transportation requests (referred to as Autonomous Mobility-on-Demand, or AMoD, system) and the electric power network. We propose a *joint* linear model that captures the coupling between the two systems stemming from the vehicles’ charging requirements. The model subsumes existing network flow models for AMoD systems and linear models for the power network, and it captures time-varying customer demand and power generation costs, road congestion, and power transmission and distribution constraints. We then leverage the linear model to jointly optimize the operation of both systems. We propose an algorithmic procedure to losslessly reduce the problem size by bundling customer requests, allowing it to be efficiently solved by state-of-the-art linear programming solvers. Finally, we study the implementation of a hypothetical electric-powered AMoD system in Dallas-Fort Worth, and its impact on the Texas power network. We show that coordination between the AMoD system and the power network can *reduce* the overall energy expenditure compared to the case where no cars are present (despite the increased demand for electricity) and yield savings of \$78M/year compared to an uncoordinated scenario. Collectively, the results of this paper provide a first-of-a-kind characterization of the interaction between electric-powered AMoD systems and the electric power network, and shed additional light on the economic and societal value of AMoD.

I. INTRODUCTION

Private vehicles are major contributors to urban pollution, which is estimated to cause over seven million premature deaths worldwide every year [1]. Plug-in electric vehicles (EVs) hold promise to significantly reduce urban pollution, both by reducing carbon dioxide emissions from internal-combustion engine vehicles, and by enabling use of renewable and low-polluting power generators as a source of energy for transportation services. However, at present, adoption of EVs for private mobility has been significantly hampered by customers’ concerns about limited range and availability of charging infrastructure.

The emerging technology of self-driving vehicles might provide a solution to these challenges and thus might represent a key enabler for the widespread adoption of EVs. Specifically, fleets of self-driving vehicles providing on-demand transportation services (referred to as Autonomous

Mobility-on-Demand, or AMoD, systems) hold promise to replace personal transportation in large cities by offering high quality of service at lower cost [2] with positive effects on safety, parking infrastructure, and congestion. Crucially, EVs are especially well-suited to AMoD systems. On the one hand, short-range trips typical of urban mobility are well-suited to the current generation of range-limited EVs; on the other hand, intelligent fleet-wide policies for rebalancing and charging can ensure that vehicles with an adequate level of charge are available to customers, virtually eliminating “range anxiety,” a major barrier to EV adoption. To fully realize this vision, however, one needs currently unavailable tools to manage the complex *couplings* between AMoD fleet management (e.g., for routing and charging the EVs) and the control of the power network. Specifically, one should consider

- 1) *Impact of transportation network on power network:* Concurrent charging of large numbers of EVs can have significant effects both on the stability of the power network and on the local price of electricity (including at the charging stations) [3], [4], [5]. For example, [5] shows that in California a 25% market penetration of (non-autonomous) EVs with fast chargers, in the absence of smart charging algorithms, would increase overall electricity demand in peak load by about 30%, and electricity prices by almost 200%.
- 2) *Impact of power network on transportation network:* Electricity prices can significantly affect travel patterns for EVs. In [4], the authors show that changes in electricity prices can radically alter the travel patterns and charging schedules of fleets of EVs in a simplified model of the San Francisco Bay Area. This, in turn, would affect electricity prices in a complex feedback loop.

The key idea behind this paper is that, by intelligently routing fleets of autonomous EVs and, in particular, by harnessing the flexibility offered by the routes and schedules for the empty-traveling vehicles, one can *actively* control such complex couplings and guarantee high-performance for the overall system (e.g., high passenger throughput and lower electricity costs). Additionally, autonomous EVs provide a unique opportunity for joint traffic and energy production management, as they could act as mobile storage devices. That is, when not used for the fulfillment of trip requests, the vehicles could be routed to target charging stations in order to either absorb excess generated energy at time of low power demand (by charging) or inject power in the power

This research was supported by the National Science Foundation under CAREER Award CMMI-1454737 and by the Toyota Research Institute (TRI). Federico Rossi and Marco Pavone are with the Department of Aeronautics & Astronautics, Stanford University, Stanford, CA 94305 {frossi2, pavone}@stanford.edu. Ramon Iglesias is with the Civil and Environmental Engineering Department, Stanford University, Stanford CA 94305, USA, rdit@stanford.edu. Mahnoosh Alizadeh is with the Electrical & Computer Engineering Department, University of California, Santa Barbara, Santa Barbara, CA 93106 alizadeh@ece.ucsb.edu

network at times of high demand (by discharging).

Literature review: The integration of *non-autonomous* EVs within the power network has been addressed in three main lines of work. A first line of work addresses the problem of scheduling charging of EVs (i.e., optimizing the charging profile in *time*) under the assumption that the vehicles' charging schedule has no appreciable effect on the power network [6], [7], [8]. This assumption is also commonly made when selecting the locations of charging stations (i.e., optimizing the charging profile in *space*) [9], [10]. A high penetration of EVs would, however, significantly affect the power network. Thus, a second line of work investigates the effects of widespread adoption of EVs on key aspects such as wholesale prices and reserve margins, for example in macroeconomic [5] and game-theoretical [3], [11] settings. Accordingly, [12], [4] investigate joint models for EV routing and power generation/distribution aimed at driving the system toward a socially-optimal solution. Finally, a third line of work investigates the potential of using EVs to regulate the power network and satisfy short-term spikes in power demand. The macroeconomic impact of such schemes (generally referred to as Vehicle-To-Grid, or V2G) has been studied in [13], where it is shown that widespread adoption of EVs and V2G technologies could foster significantly increased adoption of wind power. Going one step further, [14] proposes a unified model for EV fleets and the power network, and derives a joint dispatching and routing strategy that maximizes social welfare (i.e., it minimizes the *overall* cost borne by all participants, as opposed to maximizing individual payoffs). However, [13] does not capture the *spatial* component of the power and transportation networks, while [14] assumes that the vehicles' schedules are fixed.

The objective of this paper is to investigate the interaction between AMoD and electric power systems (jointly referred to as Power-in-the-loop AMoD, or P-AMoD, systems) in terms of modeling and algorithmic tools to effectively manage their couplings. In this context, our work improves upon the state of the art (in particular, [12], [4]) along three main dimensions: (i) it considers a fleet of *shared* and *autonomous* EVs, which offer significant additional degrees of freedom for vehicle scheduling, routing, and charging; (ii) it provides efficient algorithms that can solve large-scale problems; and (iii) it characterizes the vehicles' ability to return power to the power network through V2G schemes, and its economic benefits.

Statement of contributions: Specifically, the contribution of this paper is threefold. First, we propose a joint *linear* model for P-AMoD systems. The model captures time-varying customer demand and generation prices, congestion in the road network, power transmission constraints on the transmission lines, and transformer capacity constraints induced by the distribution network. Second, we leverage the model to design tools that optimize the operations of P-AMoD systems and, in particular, maximize social welfare. To this end, we propose an algorithmic procedure to losslessly reduce the dimensionality of the P-AMoD model. The procedure allows P-AMoD problems with hundreds of road links, time

horizons of multiple hours, and any number of customers and vehicles to be solved on commodity hardware. Third, we apply the model and algorithms to a case study of a hypothetical deployment of an AMoD system in Dallas-Fort Worth, TX. We show that coordination between the AMoD system and the electric power network can have a significant positive impact on the price of electricity (remarkably, the overall electricity expenditure in presence of the AMoD system is *lower* than in the case where no vehicles are present, despite the increased demand), while retaining *all* the convenience and sustainability benefits of AMoD. This suggests that the societal value of AMoD systems spans beyond mobility: properly coordinated, AMoD systems can deliver significant benefits to the wider community by helping increase the efficiency of the power network.

Organization: The remainder of this paper is organized as follows. In Section II we present a linear model that captures the interaction between an AMoD system and the power network. In Section III, we propose a procedure to losslessly reduce the size of the model by bundling customer requests. In Section IV, we evaluate our model and algorithm on a case study of Dallas-Fort Worth. Finally, in Section V, we draw conclusions and discuss directions for future work.

II. MODEL DESCRIPTION AND PROBLEM FORMULATION

We propose a linear, flow-based model that captures the interaction between an AMoD system and the power network. The model consists of two parts.

First, we extend the model in [15] to a time-varying network flow model of an AMoD system with EVs. We assume that a Transportation Service Operator (TSO) manages the AMoD system in order to fulfill passenger trip requests within a given road network. The road links are subject to congestion, and the trip requests arrive according to an *exogenous* dynamical process. The TSO must not only compute the routes for the autonomous EVs (i.e. *vehicle routing*), but also issue tasks and routes for empty vehicles in order to, for example, realign the fleet with the asymmetric distribution of trip demand (i.e. *vehicle rebalancing*). Due to limited battery capacity, the vehicles need to periodically charge at charging stations. The price of electricity varies between charging stations – the charging schedule is determined by the TSO in order to minimize the fleet's operational cost.

The price of electricity itself is a result of the power system operation to balance supply and demand, and varies across the power grid. Thus, we next review the linear (DC) power flow model of the power network and the economic dispatch problem. The power transmission network comprises energy providers that are connected to load buses through high-voltage transmission lines. Transmission capacities (dictated chiefly by thermal considerations) limit the amount of power that can be transferred on each transmission line. Load buses are connected to charging stations and other sources of power demand through the distribution systems: this system induces constraints on the amount of power that can be served to each load bus. Power demands other than those from charging stations are regarded as exogenous parameters in this paper.

The power network is controlled by an Independent System Operator (ISO). The ISO also determines prices at the load buses (and, consequently, at the charging stations) so as to guarantee grid reliability while minimizing the overall generation cost (a problem known as *economic dispatch*).

The vehicles' charging introduces a critical coupling between the transportation and the power networks. The loads due to charging influence the local price of electricity set by the ISO – the prices, in turn, affect the optimal charging schedule computed by the TSO. Accordingly, we conclude this section by describing the interaction between the two models, and we propose a joint model for Power-in-the-loop AMoD.

A. Network Flow Model of an AMoD system

We consider a time-varying, finite-horizon model for the AMoD system. The time horizon of the problem is discretized in T time intervals; the battery charge level of the autonomous vehicles is similarly discretized in C charge levels, each corresponding to an amount of energy denoted as J_C .

Road network: The road network is modeled as a directed graph $R = (\mathcal{V}_R, \mathcal{E}_R)$, where \mathcal{V}_R denotes the node set and $\mathcal{E}_R \subseteq \mathcal{V}_R \times \mathcal{V}_R$ denotes the edge set. Nodes $v \in \mathcal{V}_R$ denote either an intersection, a charging station, or a trip origin/destination. Edges $(v, w) \in \mathcal{E}_R$ denote the availability of a road link connecting nodes v and w . Each edge (v, w) has an associated length $d_{(v,w)} \in \mathbb{R}_{\geq 0}$, traversal time $t_{(v,w)} \in \{1, \dots, T\}$, energy requirement $c_{(v,w)} \in \{-C, \dots, C\}$, and traffic capacity $\bar{f}_{v,w} \in \mathbb{R}_{\geq 0}$. The length $d_{(v,w)}$ determines the mileage driven along the road link; the traversal time $t_{(v,w)}$ characterizes the travel time on the road link in absence of congestion; the energy requirement $c_{(v,w)}$ models the energy consumption (i.e., the number of charge levels) required to traverse the link in absence of congestion; the capacity $\bar{f}_{v,w}$ captures the maximum vehicle flow rate (i.e., the number of vehicles per unit of time) that the road link can accommodate without experiencing congestion.

Vehicles traversing the road network can recharge and discharge their batteries at charging stations, whose locations are modeled as a set of nodes $\mathcal{S} \subset \mathcal{V}_R$. Each charging station $s \in \mathcal{S}$ is characterized by a charging rate $\delta c_s^+ \in \{1, \dots, C\}$, a discharging rate $\delta c_s^- \in \{-C, \dots, -1\}$, a time-varying charging price $p_s^+(t) \in \mathbb{R}$, a time-varying discharging price $p_s^-(t) \in \mathbb{R}$, and a capacity $\bar{S}_s \in \mathbb{N}$. The charging and discharging rates δc_s^+ and δc_s^- correspond to the amount of energy (in charge levels) that the charger can provide to a vehicle (or, conversely, that a vehicle can return to the power grid) in one unit of time. For simplicity, we assume that the charging rates are fixed; however, the model can be extended to accommodate variable charging rates. The charging and discharging prices $p_s^+(t)$ and $p_s^-(t)$ capture the unit cost of energy (or, conversely, the unit payment the vehicles receive for returning power to the grid) at time t ; in this paper, $p_s^+(t) = p_s^-(t)$. The capacity \bar{S}_s models the maximum number of vehicles that can simultaneously charge or discharge at station s .

Expanded AMoD network: We introduce an *expanded* AMoD network modeled as a directed graph $G = (\mathcal{V}, \mathcal{E})$. The graph G captures the time-varying nature of the problem and tracks the battery charge level of the autonomous vehicles. Specifically, nodes $\mathbf{v} \in \mathcal{V}$ model physical locations at a given time and charge level, while edges $e \in \mathcal{E}$ model road links and charging actions at a given time and charge level. Formally, a node $\mathbf{v} \in \mathcal{V}$ corresponds to a tuple $\mathbf{v} = (v_v, t_v, c_v)$, where $v_v \in \mathcal{V}_R$ is a node in the road network graph R ; $t_v \in \{1, \dots, T\}$ is a discrete time; and $c_v \in \{1, \dots, C\}$ is a discrete charge level. The edge set \mathcal{E} is partitioned into two subsets, namely \mathcal{E}_L and \mathcal{E}_S , such that $\mathcal{E}_L \cup \mathcal{E}_S = \mathcal{E}$ and $\mathcal{E}_L \cap \mathcal{E}_S = \emptyset$. Edges $e \in \mathcal{E}_L$ represent road links, whereas edges $e \in \mathcal{E}_S$ model the charging/discharging process at the stations. An edge (\mathbf{v}, \mathbf{w}) belongs to \mathcal{E}_L when (i) an edge (v_v, v_w) exists in the road network graph edge set \mathcal{E}_R , (ii) the link $(v_v, v_w) \in \mathcal{E}_R$ can be traversed in time $t_w - t_v = t_{(v_v, v_w)}$, and (iii) the battery charge required to traverse the link is $c_v - c_w = c_{(v_v, v_w)}$. Conversely, an edge (\mathbf{v}, \mathbf{w}) represents a charging/discharging edge in \mathcal{E}_S when (i) $v_v = v_w$ is the location of a charging station in \mathcal{S} and (ii) the charging/discharging rate at the charging location v_v is $(c_w - c_v)/(t_w - t_v) = \delta c_{v_v}^+$ (charging) or $(c_w - c_v)/(t_w - t_v) = \delta c_{v_v}^-$ (discharging). Figure 1 (left) shows a graphical depiction of the graph G .

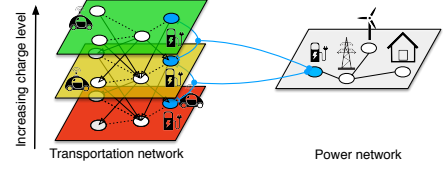


Fig. 1. Augmented transportation and power networks. Blue nodes represent charging stations: the flows on charging and discharging edges affect the load at the corresponding nodes in the power network. For simplicity, only one time step is shown.

Customer and rebalancing routes: Transportation requests are represented by the set of tuples $\{(v_m, w_m, t_m, \lambda_m)\}_{m=1}^M$, where $v_m \in \mathcal{V}_R$ is the request's origin location, $w_m \in \mathcal{V}_R$ is the request's destination location, t_m is the requested pickup time, and λ_m is the average customer arrival rate (or simply customer rate) of request m at time interval t_m . Transportation requests are assumed to be known and deterministic.

The goal of the TSO is to compute a routing and recharging policy for the self-driving vehicles. To achieve this, we model vehicle routes as network flows [16]. Network flows are an *equivalent representation* for routes. Indeed, any route can be represented as a network flow assuming value 1 on edges belonging to the route and 0 elsewhere; conversely, all network flows considered in this paper can be represented as a collection of weighed routes [16, Ch. 3]. This representation allows us to leverage the rich theory of network flows: in particular, in Section III section we exploit this theory to *losslessly reduce* the dimensionality of the optimization problem. We refer the reader to [17, Section II.B] for a thorough discussion.

We denote the *customer flow* as the rate of customer-carrying vehicles belonging to a specific transportation request $(v_m, w_m, t_m, \lambda_m)$ traversing an edge $e \in \mathcal{E}$. Formally, for transportation request m , the customer flow is a function $f_m(\mathbf{v}, \mathbf{w}) : \mathcal{E} \mapsto \mathbb{R}_{\geq 0}$, that represents the rate of customers belonging to request m traveling from location $v_{\mathbf{v}}$ to location $v_{\mathbf{w}}$ (or charging/discharging at location $v_{\mathbf{v}} = v_{\mathbf{w}}$) from time $t_{\mathbf{v}}$ to time $t_{\mathbf{w}}$, with an initial battery charge of $c_{\mathbf{v}}$ and a final battery charge of $c_{\mathbf{w}}$. Analogously, the rebalancing (or customer-empty) flow $f_0(\mathbf{v}, \mathbf{w}) : \mathcal{E} \mapsto \mathbb{R}_{\geq 0}$ represents the rate of empty vehicles traversing a road link or charging/discharging. Customer flows must satisfy a *continuity* condition: customer-carrying vehicles entering a node at a given time and charge level must exit the same node at the same time and with the same charge level. Equation (1) enforces this condition:

$$\sum_{\mathbf{u}: (\mathbf{u}, \mathbf{v}) \in \mathcal{E}} f_m(\mathbf{u}, \mathbf{v}) + 1_{v_{\mathbf{v}}=v_m} 1_{t_{\mathbf{v}}=t_m} \lambda_m^{c_{\mathbf{v}}, \text{in}} = \sum_{\mathbf{w}: (\mathbf{v}, \mathbf{w}) \in \mathcal{E}} f_m(\mathbf{v}, \mathbf{w}) + 1_{v_{\mathbf{v}}=w_m} \lambda_m^{t_{\mathbf{v}}, c_{\mathbf{v}}, \text{out}} \quad \forall \mathbf{v} \in \mathcal{V}, m \in \{1, \dots, M\}, \quad (1a)$$

$$\sum_{c=1}^C \lambda_m^{c, \text{in}} = \lambda_m, \quad \sum_{t=1}^T \sum_{c=1}^C \lambda_m^{t, c, \text{out}} = \lambda_m, \quad \forall m \in \{1, \dots, M\}. \quad (1b)$$

where the variable $\lambda_m^{c, \text{in}}$ denotes the customer rate departing with charge level c and the variable $\lambda_m^{t, c, \text{out}}$ denotes the customer rate reaching the destination at time t with charge level c ; both are optimization variables. Function 1_x denotes the indicator function of the Boolean variable $x = \{\text{true}, \text{false}\}$, that is $1_x = 1$ if x is true, and $1_x = 0$ if x is false.

Rebalancing flows must satisfy a continuity condition analogous to the one for the customer flows. In addition, rebalancing flows must satisfy a *consistency* condition representing the fact that a customer may only depart the origin location if an empty vehicle is available. Finally, the initial position and charge level of the vehicles is fixed; the final position and charge level is an optimization variable (possibly subject to constraints, e.g., on the minimum final charge level). The constraints for the initial and final positions of the rebalancing vehicles at each node $\mathbf{v} \in \mathcal{V}$ are captured by a set of functions $N_I(\mathbf{v})$ and $N_F(\mathbf{v})$, respectively. Formally, $N_I(\mathbf{v})$, with $t_{\mathbf{v}} = 0$, denotes the number of rebalancing vehicles entering the AMoD system at location $v_{\mathbf{v}}$ with charge level $c_{\mathbf{v}}$. Conversely, $N_F(\mathbf{v})$, with $t_{\mathbf{v}} = T$ denotes the number of rebalancing vehicles at location $v_{\mathbf{v}}$ with charge level $c_{\mathbf{v}}$. For $t_{\mathbf{v}} \neq 0$, $N_I(\mathbf{v}) = 0$; for $t_{\mathbf{v}} \neq T$, $N_F(\mathbf{v}) = 0$. The overall number of vehicles in the network is $\sum_{\mathbf{v} \in \mathcal{V}} N_I(\mathbf{v})$. Equation (2) simultaneously enforces the rebalancing vehicles' continuity condition, consistency condition, and the constraints on the initial and final locations:

$$\sum_{\mathbf{u}: (\mathbf{u}, \mathbf{v}) \in \mathcal{E}} f_0(\mathbf{u}, \mathbf{v}) + \sum_{m=1}^M 1_{v_{\mathbf{v}}=w_m} \lambda_m^{t_{\mathbf{v}}, c_{\mathbf{v}}, \text{out}} + N_I(\mathbf{v}) = \sum_{\mathbf{w}: (\mathbf{v}, \mathbf{w}) \in \mathcal{E}} f_0(\mathbf{v}, \mathbf{w}) + \sum_{m=1}^M 1_{v_{\mathbf{v}}=v_m} 1_{t_{\mathbf{v}}=t_m} \lambda_m^{c_{\mathbf{v}}, \text{in}} + N_F(\mathbf{v}), \quad \forall \mathbf{v} \in \mathcal{V}. \quad (2)$$

Congestion: We adopt a simple *threshold* model for congestion: the vehicle flow on each road link is constrained to be smaller than the road link's capacity. The model is analogous to the one adopted in [15] and is consistent with classical traffic flow theory [18]. This simplified congestion model is adequate for our goal of *controlling* the vehicles' routes and charging schedules, and ensures tractability of the resulting optimization problem; higher-fidelity models can be used for the *analysis* of the AMoD system's operations. Equation (3) enforces the road congestion constraint:

$$\sum_{c_{\mathbf{v}}=1}^C \sum_{m=0}^M f_m(\mathbf{v}, \mathbf{w}) \leq \bar{f}_{(v_{\mathbf{v}}, v_{\mathbf{w}})}, \quad \forall (v_{\mathbf{v}}, v_{\mathbf{w}}) \in \mathcal{E}_R, t_{\mathbf{v}} \in \{1, \dots, T\}. \quad (3)$$

Charging stations can simultaneously accommodate a limited number of vehicles. The station capacity constraint is enforced with Equation (4).

$$\sum_{\substack{(\mathbf{v}, \mathbf{w}) \in \mathcal{E}_S: \\ v_{\mathbf{v}}=v_{\mathbf{w}}=v}} \sum_{m=0}^M f_m(\mathbf{v}, \mathbf{w}) \leq \bar{S}_{v_{\mathbf{v}}}, \quad \forall v \in \mathcal{S}, t \in \{1, \dots, T\}. \quad (4)$$

Network flow model of an AMoD system: The travel time T_M experienced by customers, a proxy for customer welfare, and the overall mileage D_V driven by (both customer-carrying and empty) vehicles, a proxy for vehicle wear, are given by

$$T_M = \sum_{(\mathbf{v}, \mathbf{w}) \in \mathcal{E}} t_{\mathbf{v}, \mathbf{w}} \sum_{m=1}^M f_m(\mathbf{v}, \mathbf{w}),$$

$$D_V = \sum_{(\mathbf{v}, \mathbf{w}) \in \mathcal{E}} d_{v_{\mathbf{v}}, v_{\mathbf{w}}} \sum_{m=0}^M f_m(\mathbf{v}, \mathbf{w}),$$

Note that T_M only includes the travel time of *customer-carrying* vehicles, whereas D_V includes the distance traveled by *all* vehicles. Also note that, for charging edges, $d_{v_{\mathbf{v}}, v_{\mathbf{w}}} = 0$. The overall cost of electricity incurred by the vehicles (including any credit from selling electricity to the power network) is

$$V_E = \sum_{(\mathbf{v}, \mathbf{w}) \in \mathcal{E}_S} \sum_{m=0}^M f_m(\mathbf{v}, \mathbf{w}) p_{(\mathbf{v}, \mathbf{w})},$$

where $p_{(\mathbf{v}, \mathbf{w})} = p_{v_{\mathbf{v}}}^+$ if $c_{\mathbf{w}} > c_{\mathbf{v}}$, $p_{(\mathbf{v}, \mathbf{w})} = p_{v_{\mathbf{v}}}^-$ otherwise.

The goal of the TSO is to solve the Vehicle Routing and Charging problem, that is, to minimize the aggregate societal cost borne by the AMoD users while satisfying all operational constraints. We define the customers' value of time (i.e., the monetary loss associated with traveling for one unit of time) as V_T and the operation cost per kilometer of the vehicles (including maintenance but excluding electricity costs) as V_D . The aggregate societal cost experienced by the AMoD users is then defined as

$$V_D D_V + V_E + V_T T_M. \quad (5)$$

The Vehicle Routing and Charging problem entails minimizing (5) subject to constraints (1), (2), (3), and (4).

B. Linear model of power network

In this paper, the power network is modeled according to the well-known DC model [19, Ch. 6], which, by assuming constant voltage magnitudes and determining the power flow on transmission lines solely based on voltage phase angles, represents an approximation to the higher-fidelity AC flow model [20].

In analogy with the treatment of the AMoD model, we discretize the time horizon of the problem in T time steps. The power grid is modeled as an undirected graph $P = (\mathcal{B}, \mathcal{E}_P)$, where \mathcal{B} is the node set, commonly referred to as buses in the power engineering literature, and $\mathcal{E}_P \subseteq \mathcal{B} \times \mathcal{B}$ is the edge set, representing the transmission lines. The subsets of buses representing generators and loads are defined as $\mathcal{G} \subset \mathcal{B}$ and $\mathcal{L} \subset \mathcal{B}$, respectively. Nodes that are neither loads nor generators are referred to as interconnects. Generators produce power and deliver it to the network, while loads absorb power from the network. Each generator $g \in \mathcal{G}$ is characterized by a maximum output power $\bar{p}_g(t)$, a minimum output power $\underline{p}_g(t)$, a unit generation cost $o_g(t)$, and maximum ramp-up and ramp-down rates $p_g^+(t)$ and $p_g^-(t)$, respectively. Transmission lines $e \in \mathcal{E}_P$ are characterized by a reactance x_e and a maximum allowable power flow \bar{p}_e (due chiefly to thermal constraints). The reactance and the maximum allowable power flow do not vary with time. Each load node $l \in \mathcal{L}$ is characterized by a required power demand $d_l(t)$. The distribution network is not modeled explicitly; however, thermal constraints due to the distribution substation transformers are modeled by an upper bound $\bar{d}_l(t)$ on the power that can be delivered at each load node.

We define a generator power function $p : (\mathcal{G}, \{1, \dots, T\}) \mapsto \mathbb{R}_{\geq 0}$, and a phase angle function $\theta : (\mathcal{B}, \{1, \dots, T\}) \mapsto \mathbb{R}$. The Economic Dispatch problem entails minimizing the generation cost subject to a set of feasibility constraints [19], namely:

$$\underset{p, \theta}{\text{minimize}} \quad \sum_{t=1}^T \sum_{g \in \mathcal{G}} o_g(t) p(g, t), \quad (6a)$$

$$\text{subject to} \quad \sum_{(u,v) \in \mathcal{E}_P} \frac{\theta(u, t) - \theta(v, t)}{x_{u,v}} + 1_{v \in \mathcal{G}} p(v, t) = 1_{v \in \mathcal{L}} d_v(t) + \sum_{(v,w) \in \mathcal{E}_P} \frac{\theta(v, t) - \theta(w, t)}{x_{v,w}}, \quad \forall v \in \mathcal{B}, t \in \{1, \dots, T\}, \quad (6b)$$

$$-\bar{p}_{b_1, b_2} \leq \frac{\theta(b_1, t) - \theta(b_2, t)}{x_{b_1, b_2}} \leq \bar{p}_{b_1, b_2}, \quad \forall (b_1, b_2) \in \mathcal{E}_P, t \in \{1, \dots, T\}, \quad (6c)$$

$$\underline{p}_g(t) \leq p(g, t) \leq \bar{p}_g(t), \quad \forall g \in \mathcal{G}, t \in \{1, \dots, T\}, \quad (6d)$$

$$-p_g^-(t) \leq p(g, t+1) - p(g, t) \leq p_g^+(t), \quad \forall g \in \mathcal{G}, t \in \{1, \dots, T-1\}, \quad (6e)$$

$$d_l(t) \leq \bar{d}_l(t), \quad \forall l \in \mathcal{L}, t \in \{1, \dots, T\}. \quad (6f)$$

Equation (6b) enforces power balance at each bus based on the so-called DC power flow equations; Equation (6c) encodes the transmission lines' thermal constraints; Equation

(6d) encodes the generation capacity constraints; Equation (6e) encodes the ramp-up and ramp-down constraints; and Equation (6f) encodes the thermal constraints of substation transformers at load nodes.

The unit price of electricity at the load nodes is typically determined through a mechanism known as Location Marginal Pricing (LMP) [19], [21]. The LMP at a node is defined as the *marginal cost* of delivering one unit of power at the node while respecting all the system constraints. It can be shown [19] that the LMP at each bus equals the dual variable corresponding to the power injection constraint (6b) at the same bus in the Economic Dispatch problem.

C. Power-in-the-loop AMoD system

The vehicles' charging requirements introduce a *coupling* between the AMoD system and the power network, as shown in Figure 1. Specifically, the vehicles' charging schedule produces a load on the power network. Such a load on the power network affects the solution to the ISO's Economic Dispatch problem and, as a result, the locational marginal prices. The change in locational marginal prices, in turn, has an effect on the TSO's optimal charging schedule. In absence of coordination, this feedback loop can lead to system instability, as shown for the case of privately-owned, non-autonomous EVs in [4].

In this section, we formulate a *joint model* for the TSO's Vehicle Routing and Charging problem and the ISO's Economic Dispatch problem. The goal of this model is to maximize the social welfare by minimizing the total cost of mobility (a profit-maximizing formulation would be similar) and the total cost of power generation and transmission. While the resulting solution is not directly actionable (since it requires the TSO and the ISO to coordinate and share their private information), coordination mechanisms can be designed to steer the system towards the optimum: we briefly discuss such mechanisms at the end of this section.

The coupling between the AMoD model and the electric power model is mediated by the charging stations. A given charging station is represented both by a node $v \in \mathcal{V}_R$ in the road network and by a load node $l \in \mathcal{L}$ in the power network. To capture this correspondence, we define an auxiliary function $\mathcal{M}_{PR} : \mathcal{L} \mapsto \{\mathcal{V}_R \cup \emptyset\}$. Given a load node $b \in \mathcal{L}$, $\mathcal{M}_{PR}(b)$ denotes the node in \mathcal{V}_R (if any) that represents a charging station connected to b . We then define two additional functions, $\mathcal{M}_{PG}^+ : (\mathcal{L}, \{1, \dots, T\}) \mapsto \{\mathcal{E} \cup \emptyset\}$ and $\mathcal{M}_{PG}^- : (\mathcal{L}, \{1, \dots, T\}) \mapsto \{\mathcal{E} \cup \emptyset\}$. The function \mathcal{M}_{PG}^+ (resp. \mathcal{M}_{PG}^-) maps a load node l and a time t to the set of charge (resp. discharge) edges in G corresponding to station $\mathcal{M}_{PR}(l)$ at time t . Formally,

$$\mathcal{M}_{PG}^+(l, t) : \{(\mathbf{v}, \mathbf{w}) \in \mathcal{E} | v_{\mathbf{v}} = v_{\mathbf{w}}, v_{\mathbf{v}} \in \mathcal{M}_{PR}(l), c_{\mathbf{v}} < c_{\mathbf{w}}, t_{\mathbf{v}} \leq t < t_{\mathbf{w}}\},$$

$$\mathcal{M}_{PG}^-(l, t) : \{(\mathbf{v}, \mathbf{w}) \in \mathcal{E} | v_{\mathbf{v}} = v_{\mathbf{w}}, v_{\mathbf{v}} \in \mathcal{M}_{PR}(l), c_{\mathbf{v}} > c_{\mathbf{w}}, t_{\mathbf{v}} \leq t < t_{\mathbf{w}}\}.$$

The load at a load bus l can be expressed as the sum of two components: an exogenous demand $d_{l,e}$ and the load due to the charger or chargers connected to that bus, quantitatively,

$$d_l(t) = d_{l,e}(t) + J_C \delta c_{\mathcal{M}_{PR}(l)}^+ \sum_{(\mathbf{v}, \mathbf{w}) \in M_{P,G}^+(l,t)} \sum_{m=0}^M f_m(\mathbf{v}, \mathbf{w}) \\ + J_C \delta c_{\mathcal{M}_{PR}(l)}^- \sum_{(\mathbf{v}, \mathbf{w}) \in M_{P,G}^-(l,t)} \sum_{m=0}^M f_m(\mathbf{v}, \mathbf{w}), \\ \forall l \in \mathcal{L}, t \in \{1, \dots, T\}. \quad (7)$$

We are now in a position to state the Power-in-the-loop AMoD (P-AMoD) problem:

$$\begin{aligned} & \underset{f_m, \lambda_m^{c,in}, \lambda_m^{c,t,out}, N_F, \theta, p}{\text{minimize}} && V_T T_M + V_D D_v + \sum_{t=1}^T \sum_{g \in \mathcal{G}} o_g(t) p(g, t), \quad (8) \\ & \text{subject to} && (1), (2), (3), (4), (6), \text{ and } (7). \end{aligned}$$

D. Discussion

Some comments are in order. The model assumes that the TSO and the ISO share the goal of maximizing social welfare and are willing to collaborate on a joint policy. This assumption is, in general, not realistic: not only do the TSO and ISO have different goals, but they are also generally reluctant to share the information required for successful coordination. However, once a socially optimal strategy is found, efficient coordination mechanisms can be designed that steer rational agents towards that strategy [22, Ch. 10]. In particular, in [4], the authors propose distributed *privacy-preserving* mechanisms that an ISO and a TSO can adopt to reach a socially-optimal equilibrium: such mechanisms can be applied to the model in this paper to steer a rational ISO and a rational TSO towards the optimal solution.

The network flow model has some well-known limitations: chiefly, it does not capture the stochasticity of the customer arrival process, and it does not directly yield *integral* routes suitable for real-time control of vehicles. Furthermore, in this paper, customer requests are assumed to be deterministic and known in advance, an assumption that is not consistent with the paradigm of on-demand mobility. However, future requests may be interpreted as the *expected* number of future transportation requests (which may be learned from historical data and demand models). Accordingly, the model proposed in this paper may be used for planning on timescales of days and hours, akin to the Day-Ahead-Market already in use in the electric power network [19]; its solution (specifically, the charge level of the vehicles and the location of empty vehicles) may be used as a *reference* for a lower-level, real-time, model predictive controller.

Finally, the DC model for the power network has some shortcomings, chiefly the inability to handle voltage constraints [23] and system-dependent accuracy [24]. On the other hand, its linearity makes it amenable to large-scale optimization and easy to integrate within the economic theory upon which the transmission-oriented market design is based on [24]. Moreover, the DC model is widely adopted among ISOs [25], and its locational marginal pricing calculations

are fairly accurate [26]. Hence, the DC model is appropriate for high-level synthesis of joint control policies such as those considered in this paper.

III. SOLUTION ALGORITHMS

The number of variables of the P-AMoD problem (8) is $(M+1)|\mathcal{E}| + MC(T+1) + T(|\mathcal{G}| + |\mathcal{E}_p| + |\mathcal{B}|)$. The size of the edge set \mathcal{E} is $|\mathcal{E}| = \Theta((|\mathcal{E}_R| + |\mathcal{S}|)CT)$, and the number of customer demands admits an upper bound $M = O(|\mathcal{V}_R|^2 T)$, since each customer demand is associated with an origin, a destination, and a departure time. Generally, the size of the problem is dominated by the variables representing customer flows in the road network – the number of such variables is $M|\mathcal{E}| = O((|\mathcal{V}_R|^2 T)(|\mathcal{E}_R| + |\mathcal{S}|)CT)$. Consider a typical problem with 100 road nodes, 300 road links, 25 charge levels, and a time horizon of 20 time steps. Such problem results in a number of variables on the order of $3 \cdot 10^{10}$, which can not be solved even by state-of-the-art solvers on modern hardware [27].

In this section, we propose a *bundling* procedure that collects multiple customer demands in a single customer flow without loss of information. The procedure allows one to reduce the number of network flows to $O(|\mathcal{V}_R|)$: as a result, the size of the prototypical problem above is reduced to $1.5 \cdot 10^7$ variables, within reach of modern solvers. The procedure relies on the notion of *bundled customer flow*,

Definition III.1 (Bundled customer flow). *Consider the set of customer requests $\{v_m, w_m, t_m, \lambda_m\}_{m=1}^M$. Denote the set of customer destinations as $\mathcal{D} := \{\cup_{m=1}^M w_m\}$. For a given destination $d_B \in \mathcal{D}$, we define a bundled customer flow as a function $f_{B,d_B}(\mathbf{u}, \mathbf{v}) : \mathcal{E} \mapsto \mathbb{R}_{\geq 0}$ that satisfies*

$$\sum_{\mathbf{u}:(\mathbf{u}, \mathbf{v}) \in \mathcal{E}} f_{B,d_B}(\mathbf{u}, \mathbf{v}) + \sum_{\substack{m \in \{1, \dots, M\}: \\ w_m = d_B}} 1_{v_{\mathbf{v}} = v_m} 1_{t_{\mathbf{v}} = t_m} \lambda_m^{c_{\mathbf{v}}, in} \\ = \sum_{\mathbf{w}:(\mathbf{v}, \mathbf{w}) \in \mathcal{E}} f_{B,d_B}(\mathbf{v}, \mathbf{w}) + \sum_{\substack{m \in \{1, \dots, M\}: \\ w_m = d_B}} 1_{v_{\mathbf{v}} = w_m} \lambda_m^{t_{\mathbf{v}}, c_{\mathbf{v}}, out}, \quad \forall \mathbf{v} \in \mathcal{V}, \quad (9a)$$

$$\sum_{c=1}^C \lambda_m^{c, in} = \lambda_m, \quad \forall m \in \{1, \dots, M\} : w_m = d_B, \quad (9b)$$

$$\sum_{t=1}^T \sum_{c=1}^C \lambda_m^{t, c, out} = \lambda_m, \quad \forall m \in \{1, \dots, M\} : w_m = d_B. \quad (9c)$$

Intuitively, the bundled customer flow for a given destination d_B can be thought of as the sum of customer flows (i.e., network flows satisfying Eq. (1)) for *all* customer requests whose destination is node d_B . A bundled customer flow is an *equivalent representation* for a set of customer flows belonging to customer requests sharing the same destination. The next lemma formalizes this intuition.

Lemma III.2 (Equivalency between customer flows and bundled customer flows). *Consider a network $G(\mathcal{V}, \mathcal{E})$ and a set of customer requests $\{v_m, w_m, t_m, \lambda_m\}_{m=1}^M$. Assume there exists a bundled customer flow $\{f_{B,d_B}(\mathbf{u}, \mathbf{v})\}_{(\mathbf{u}, \mathbf{v}) \in \mathcal{E}}$*

that satisfies Equation (9) for a destination $d_B \in \mathcal{D}$. Then, for each customer request $\{v_m, d_B, t_m, \lambda_m\}$ with destination d_B , there exists a customer flow $f_m(\mathbf{u}, \mathbf{v})$ that satisfies Eq. (1). Furthermore, for each edge $(\mathbf{u}, \mathbf{v}) \in \mathcal{E}$, $f_{B,d_B}(\mathbf{u}, \mathbf{v}) = \sum_{m \in \{1, \dots, M\}: w_m = d_B} f_m(\mathbf{u}, \mathbf{v})$.

Proof sketch: The proof is constructive. Define as path flow a network flow that has a fixed intensity on edges belonging to a path without cycles from the origin to the destination and zero otherwise. The flow decomposition algorithm [16, Ch. 3.5] is used to decompose the bundled customer flow into a collection of path flows, each with a single origin node $\mathbf{v} \in \mathcal{V}$ and destination node $\mathbf{w} \in \mathcal{V}$ with $v_w = d_B$. The customer flow for customer request (v_m, d_B, t, λ) is then obtained as the sum of path flows leaving origin nodes $\{\mathbf{v} = (v_m, t_m, c)\}_{c=1}^C$ with total intensity λ_m .

We can leverage the result in Lemma III.3 to solve the P-AMoD problem in terms of bundled customer flows, thus dramatically decreasing the problem size. The next theorem formalizes this intuition.

Theorem III.3 (P-AMoD with bundled customer flows). *Consider the following problem, referred to as the bundled P-AMoD problem:*

$$\begin{aligned} & \underset{f_0, f_{B,d_B}, \lambda_m^{c,in}, \lambda_m^{c,out}, N_F, \theta, p}{\text{minimize}} && \sum_{m=1}^M V_T T_M + V_D D_v + \sum_{t=1}^T \sum_{g \in \mathcal{G}} o_g(t) p(g, t), \quad (10) \\ & \text{subject to} && (9) \quad \forall d_B \in \mathcal{D}, \\ & && (2), (3), (4), (6), \text{ and } (7), \end{aligned}$$

where each instance of $\sum_{m=1}^M f_m$ in the cost function and in Equations (2), (3), (4), (6), and (7) is replaced by $\sum_{d_B \in \mathcal{D}} f_{B,d_B}$. The bundled P-AMoD problem (10) admits a feasible solution if and only if the P-AMoD problem (8) admits a solution. Furthermore, the optimal values of Problem (8) and Problem (10) are equal.

Proof. (i) The bundled P-AMoD problem admits a solution if the P-AMoD problem admits a solution. Consider a solution to the P-AMoD problem. For each destination node, define the bundled flow as the sum of the customer flows for customers directed to that destination:

$$f_{B,d_B} = \sum_{m: w_m = d_B} f_m \quad \forall d_B \in \mathcal{B}.$$

It is easy to verify that the resulting network flow satisfies Eq. (9). Also, the customer flows satisfy Equations (2), (3), (4), (6), and (7) and, for every edge, by construction $\sum_{d_B \in \mathcal{B}} f_{B,d_B} = \sum_{d_B \in \mathcal{B}} \sum_{m: w_m = d_B} f_m = \sum_m f_m$. Therefore the set of bundled customer flows $\{f_{B,d_B}\}_{d_B \in \mathcal{D}}$ satisfies Equations (2), (3), (4), (6), and (7) where each instance of $\sum_{m \in [1, M]} f_m$ is replaced by $\sum_{d_B \in \mathcal{D}} f_{B,d_B}$.

(ii) The P-AMoD problem admits a solution if the bundled P-AMoD problem admits a solution. Lemma 1 shows that, if there exists a set of bundled flows that satisfy Problem (10), then there exists a set of customer flows that satisfy Equation (1). Furthermore, for each edge, $\sum_m f_m = \sum_{d_B \in \mathcal{B}} f_{B,d_B}$.

Since the bundled flows satisfies the modified version of Equations (2), (3), (4), (6), and (7), the customer flows also satisfy them.

(iii) The bundled P-AMoD problem and the P-AMoD problem have the same cost. Due to Lemma 1, $\sum_m f_m = \sum_{d_B \in \mathcal{B}} f_{B,d_B}$. The claim follows from the definition of the cost in Problem (10). \square

The number of variables in Problem (10) is $O((|\mathcal{V}_R| + 1)|\mathcal{E}| + |\mathcal{V}_R|C(T+1) + T(|\mathcal{G}| + |\mathcal{E}_p| + |\mathcal{B}|))$. The number of variables grows quadratically with the number of nodes in the road network, and grows linearly with the number of edges in the road network, the time horizon, the number of charge levels, and the number of nodes, edges, and generators in the power network. Crucially, the size of Problem (10) does not depend on the number of customer requests.

IV. NUMERICAL EXPERIMENTS

We study a hypothetical deployment of an AMoD system to satisfy medium-distance commuting needs in the Dallas-Fort Worth metroplex, with the primary objective of investigating the interaction between such system and the Texas power network. Specifically, we study a nine-hour interval corresponding to one commuting cycle, from 5:30 a.m. to 2:30 p.m., with 30-minute resolution. Data on commuting patterns is collected from the Census Transportation Planning Products (CTPP) 2006-2010 Census Tract Flows, based on the American Communities Survey (ACS) [28]. Departure times are gathered from ACS data [29]. Census tracts in the metroplex are aggregated in 25 clusters, as shown in Figure 2. We only consider trips starting and ending in different clusters: the total number of customer requests is 218,472. The commuters' value of time is set equal to \$24.40/hr, in accordance with DOT guidelines [30].

The road network, the road capacities, and the travel times are obtained from OpenStreetMap data [31], [32] and simplified. The resulting road network, containing 25 nodes and 147 road links, is shown in Figure 2.

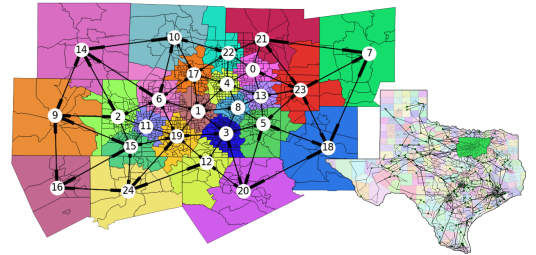


Fig. 2. Census tracts and simplified road network for Dallas-Fort Worth, and Texas power network. The capacity of each edge equals the overall capacity of roads connecting the start and end clusters. The travel time between two nodes is the minimal travel time between the centroids of the corresponding clusters.

The battery capacity and power consumption of the EVs are modeled after the 2017 Chevrolet Bolt EV [33]. The cost of operation of the vehicles, excluding electricity costs, is 48.6c/mile, in accordance with DOT guidelines [34]. The fleet consists of 100,000 vehicles, i.e. 1 AMoD vehicle for every 2.2 customers, similar to the 2.6 ratio in [2]. To

represent the possibility that vehicles might not begin the day fully charged, each vehicle starts the day with a 50% battery charge and is required to have the same level of charge at the end of the simulation.

We adopt a synthetic model of the Texas power network provided in [35] and portrayed in Figure 2. The model provided does not contain power generation costs: we labeled each generator according to its source of power and assigned generation costs according to U.S. Energy Information Administration estimates [36]. Furthermore, the model is time-invariant; to model the time evolution of power loads and the availability of solar and wind power we used historical data from ERCOT, Texas’s ISO [37], and we imposed ramp-up and ramp-down constraints of 10%/hr and 40%/hr on the generation capability of nuclear and coal power plants, respectively.

We compare the results of three simulation studies. In the baseline simulation study, no electric vehicles are present: we consider the power network *in isolation* subject only to exogenous loads. In the P-AMoD simulation study, we solve Problem (10), which embodies the cooperation between the TSO and the ISO. Finally, in the uncoordinated simulation study, we first solve the TSO’s Vehicle Routing and Charging problem with *fixed* electricity prices obtained from the baseline simulation study; we then compute the load on the power network resulting from the vehicles’ charging and discharging; finally, we solve the ISO’s Economic Dispatch problem with a power load corresponding to the sum of the exogenous load and the load due to the AMoD system. The uncoordinated simulation study captures the scenario where the TSO attempts to minimize its passengers’ social cost while disregarding the coupling with the power network.

Table I and Figure 3 show the results. The quality of

TABLE I
SIMULATION RESULTS (ONE COMMUTING CYCLE, 9 HOURS).

	Baseline	P-AMoD	Noncoop.
Avg. cust. travel time [h]	-	1.0582	1.0561
Tot. energy demand [GWh]	459.471	460.636	460.623
Tot. electricity expenditure [k\$]	35,588.25	35,515.44	35,671.51
w.r.t. baseline [k\$]		-72.80	+83.26
Avg. price in DFW [\$ / MW]	81.09	80.12	81.02
TSO tot. elec. expenditure [k\$]	-	81.33	89.22

service experienced by TSO customers, measured by the average travel time, is virtually identical in the P-AMoD and in the uncoordinated case. The energy demand of the AMoD system is also very similar in both cases. On the other hand, the effect of coordination on the overall electricity expenditure is noticeable. Coordination between the TSO and the ISO causes a *reduction* in the total expenditure for electricity of \$72,800 per commuting cycle compared to the baseline case, despite the increased demand! In other words, a P-AMoD system allows a TSO to deliver on-demand transportation without an increase in overall electricity expenditure – a remarkable, and perhaps surprising finding. Instead, in the uncoordinated case, the total expenditure

for electricity is *increased* by \$83,260. This corresponds to a difference of \$156,060 between the P-AMoD case and the uncoordinated case, which compounds to savings in electricity expenditure of \$78M per year (assuming two commuting cycles per day and 250 work days per year).

Who benefits from the reduction in energy expenditure? From the last two rows in Table I, one can see that the average price of electricity in the P-AMoD case is 1.1% lower than in the uncoordinated case in Dallas-Fort Worth (corresponding to savings of \$61.2M/year). The energy expenditure of the TSO in the P-AMoD case is 8.8% lower than in the uncoordinated case (a saving of \$7,890 per commuting cycle, corresponding to close to \$4M/year). Finally, electricity customers outside of Dallas experience a minimal reduction of 0.11% in their energy expenditure. Thus, the majority of the benefits of coordination are reaped by customers of the power network in the region where the AMoD system is deployed; the TSO also benefits from a noticeable reduction in its electricity expenditure.

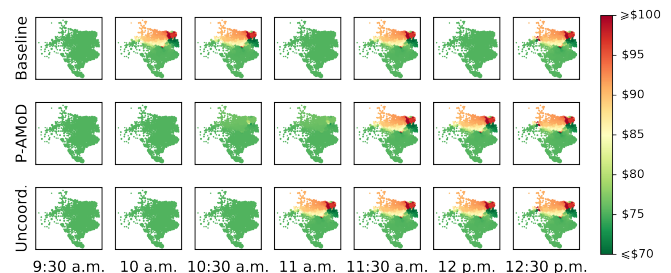


Fig. 3. LMPs in Texas between 9:30 a.m. and 12:30 p.m. The color of each dot denotes the price of electricity; dot size denotes power demand. The presence of the AMoD fleet can reduce locational marginal prices; coordination between the TSO and the ISO can yield a further reduction.

Figure 3 shows this phenomenon in detail. The presence of the AMoD system results in a decrease in the LMPs with respect to the baseline case (10 a.m. and 10:30 a.m.). As electricity prices increase, empty vehicles travel to carefully chosen stations to sell their stored energy back to the network: this results in reduced congestion and lower prices in the power network, even in the absence of coordination. Crucially, coordination between the TSO and the ISO can result in further decreases in the price of electricity with respect to the uncoordinated case (11 a.m.), significantly curtailing the impact of the AMoD system on the power network. By leveraging their battery capacities and acting as mobile storage units, the EVs are able to reduce congestion in the power transmission network: this results in lower LMPs in the Dallas-Fort Worth region, and hence lower electricity expenditure. Simulations were carried out on commodity hardware (Intel Core i7-5960, 64 GB RAM) and used the MOSEK LP solver. The simulations required 1,222s for the P-AMoD scenario, 715s for the uncoordinated scenario, and 7.12s for the baseline scenario.

V. CONCLUSIONS AND FUTURE WORK

In this paper we studied the interaction between an AMoD system and the power network. The linear model

we proposed subsumes earlier models for AMoD systems and for the power network; critically, the model captures the coupling between the two systems and allows for their *joint optimization*. We also proposed a numerical procedure to losslessly reduce the dimensionality of the P-AMoD optimization problem (Eq. (10)), making realistic problems amenable to efficient numerical optimization on commodity hardware. We applied our model to a case study of an AMoD deployment in Dallas-Fort Worth, TX. The case study showed that coordination between the TSO and the ISO can result in a *reduction* in the overall electricity expenditure (despite the increase in demand), while having a negligible impact on the TSO's quality of service.

This work opens the field to many future avenues of research. First, the model in this paper assumes that the TSO and ISO are willing to collaborate and to share their private information. Future research will explore the use of distributed optimization algorithms, with a specific focus on privacy-preserving algorithms. Second, we wish to improve applicability of our model to stochastic customer demand and power loads, achieve frequency of control at the sub-second level, and improve geographic granularity up to the city block level. Thus, we will explore simplified models that are amenable to real-time implementation and leverage model-predictive control techniques to synthesise real-time control and coordination algorithms. Third, the model of the power network considered in this paper does not capture ancillary services such as regulation and spinning reserves. We will extend our model to capture those and evaluate the feasibility of using coordinated fleets of EVs to aid in short-term control of the power network. Finally, we wish to explore the effect of TSO-ISO coordination on penetration of renewable energy sources, and to determine whether large-scale deployment of AMoD systems can increase the fraction of renewable power sources in the generation power mix.

REFERENCES

- [1] World Health Organization (WHO). (2014) 7 million premature deaths annually linked to air pollution. <http://www.who.int/mediacentre/news/releases/2014/air-pollution/en/>. World Health Organization (WHO).
- [2] K. Spieser, K. Treleaven, R. Zhang, E. Frazzoli, D. Morton, and M. Pavone, "Toward a systematic approach to the design and evaluation of Autonomous Mobility-on-Demand systems: A case study in Singapore," in *Road Vehicle Automation*. Springer, 2014.
- [3] R. Sioshansi, "OR Forum—modeling the impacts of electricity tariffs on plug-in hybrid electric vehicle charging, costs, and emissions," *Operations Research*, vol. 60, no. 3, pp. 506–516, 2012.
- [4] M. Alizadeh, H.-T. Wai, M. Chowdhury, A. Goldsmith, A. Scaglione, and T. Javidi, "Joint management of electric vehicles in coupled power and transportation networks," *IEEE Transactions on Control of Network Systems*, 2016, in press.
- [5] S. W. Hadley and A. A. Tsvetkova, "Potential impacts of plug-in hybrid electric vehicles on regional power generation," *The Electricity Journal*, vol. 22, no. 10, pp. 56–68, 2009.
- [6] N. Rotering and M. Ilic, "Optimal charge control of plug-in hybrid electric vehicles in deregulated electricity markets," *IEEE Transactions on Power Systems*, vol. 26, no. 3, pp. 1021–1029, 2011.
- [7] K. Turitsyn, N. Sinitsyn, S. Backhaus, and M. Chertkov, "Robust broadcast-communication control of electric vehicle charging," in *IEEE International Conference on Smart Grid Communications (SmartGridComm)*, 2010.
- [8] W. Tushar, W. Saad, H. V. Poor, and D. B. Smith, "Economics of electric vehicle charging: A game theoretic approach," *IEEE Transactions on Power Systems*, vol. 3, no. 4, pp. 1767–1778, 2012.
- [9] D. Goeke and M. Schneider, "Routing a mixed fleet of electric and conventional vehicles," *European Journal of Operational Research*, vol. 245, no. 1, pp. 81–99, 2015.
- [10] S. Pourazarm, C. G. Cassandras, and T. Wang, "Optimal routing and charging of energy-limited vehicles in traffic networks," *Int. Journal of Robust and Nonlinear Control*, vol. 26, no. 6, pp. 1325–1350, 2016.
- [11] L. Wang, A. Lin, and Y. Chen, "Potential impact of recharging plug-in hybrid electric vehicles on locational marginal prices," *Naval Research Logistics*, vol. 57, no. 8, pp. 686–700, 2010.
- [12] M. Alizadeh, H.-T. Wai, A. Scaglione, A. Goldsmith, Y. Y. Fan, and T. Javidi, "Optimized path planning for electric vehicle routing and charging," in *Allerton Conf. on Communications, Control and Computing*, 2014.
- [13] W. Kempton and J. Tomić, "Vehicle-to-grid power fundamentals: Calculating capacity and net revenue," *Journal of Power Sources*, vol. 144, no. 1, pp. 268–279, 2005.
- [14] M. E. Khodayar, L. Wu, and Z. Li, "Electric vehicle mobility in transmission-constrained hourly power generation scheduling," *IEEE Transactions on Smart Grid*, vol. 4, no. 2, pp. 779–788, 2013.
- [15] R. Zhang, F. Rossi, and M. Pavone, "Routing autonomous vehicles in congested transportation networks: Structural properties and coordination algorithms," in *Robotics: Science and Systems*, 2016.
- [16] R. K. Ahuja, T. L. Magnanti, and J. B. Orlin, *Network Flows: Theory, Algorithms and Applications*. Prentice Hall, 1993.
- [17] F. Rossi, R. Iglesias, R. Zhang, and M. Pavone. (2017) Congestion-aware randomized routing in autonomous mobility-on-demand systems. Extended version available at <https://asl.stanford.edu/wp-content/papercite-data/pdf/Rossi.Iglesias.Zhang.Pavone.CDC17.pdf>.
- [18] J. G. Wardrop, "Some theoretical aspects of road traffic research," *Proceedings of the Institution of Civil Engineers*, vol. 1, no. 3, pp. 325–362, 1952.
- [19] D. S. Kirschen and G. Strbac, *Fundamentals of Power System Economics*, 1st ed. John Wiley & Sons, 2004.
- [20] J. Glover, M. Sarma, and T. Overbye, *Power System Analysis and Design*, 5th ed. Cengage Learning, 2011.
- [21] H. Liu, L. Tesfatsion, and C. A. A., "Derivation of locational marginal prices for restructured wholesale power markets," *Journal of Energy Markets*, vol. 2, no. 1, pp. 3–27, 2009.
- [22] Y. Shoham and K. Leyton-Brown, *Multiagent Systems*. Cambridge University Press, 2008.
- [23] W. W. Hogan, "Markets in real electric networks require reactive prices," in *Electricity Transmission Pricing and Technology*. Dordrecht: Springer Netherlands, 1996, ch. 7.
- [24] B. Stott, J. Jardim, and O. Alsaç, "DC power flow revisited," *IEEE Transactions on Power Systems*, vol. 24, no. 3, pp. 1290–1300, 2009.
- [25] R. P. O'Neill, T. Dautel, and E. Krall, "Recent ISO software enhancements and future software and modeling plans," Federal Energy Regulatory Commission, Tech. Rep., 2011.
- [26] T. J. Overbye, X. Cheng, and Y. Sun, "A comparison of the AC and DC power flow models for LMP calculations," in *Hawaii International Conference on System Sciences*, 2004.
- [27] H. D. Mittelmann. (2016) Decision tree for optimization software. [Online]. Available: <http://plato.asu.edu/guide>
- [28] Federal Highway Administration, "Census Transportation Planning Products (CTTP) 2006-2010 Census Tract Flows," U.S. Department of Transportation, Tech. Rep., 2014. [Online]. Available: https://www.fhwa.dot.gov/planning/census_issues/cttp/data_products/2006-2010-tract.flows/
- [29] United States Census Bureau. (2017) American Community Survey. Commuting in the United States: 2009. Supplemental Table B: Time of Departure. Available at <https://www.census.gov/hhes/commuting/data/commuting.html>.
- [30] U.S. Department of Transportation, "Revised departmental guidance on valuation of travel time in economic analysis," Tech. Rep., 2015.
- [31] M. Haklay and P. Weber, "OpenStreetMap: User-generated street maps," *IEEE Pervasive Computing*, vol. 7, no. 4, pp. 12–18, 2008.
- [32] G. Boeing, "OSMnx: New methods for acquiring, constructing, analyzing, and visualizing complex street networks," *Computers, Environment and Urban Systems*, 2017, forthcoming.
- [33] Chevrolet. (2017) Bolt EV. Available at <http://www.chevrolet.com/bolt-ev-electric-vehicle>.

- [34] Bureau of Transportation Statistics, "National transportation statistics." U.S. Department of Transportation, Tech. Rep., 2016.
- [35] Illinois Center for a Smarter Electric Grid (ICSEG). (2016) Texas 2000-June 2016 synthetic power case. Information Trust Institute, University of Illinois at Urbana-Champaign, Coordinated Science Laboratory. [Online]. Available: <http://icseg.iti.illinois.edu/synthetic-power-cases/texas2000-june2016/>
- [36] EIA, "Levelized cost and levelized avoided cost of new generation resources in the annual energy outlook 2017," U.S. Energy Information Administration, Tech. Rep., 2017.
- [37] Electric Reliability Council of Texas (ERCOT). (2017) Grid information. Available at <http://www.ercot.com/gridinfo/>.